



J. Serb. Chem. Soc. 76 (11) 1537–1550 (2011)
JSCS-4227

Journal of the Serbian Chemical Society

JSCS-info@shd.org.rs • www.shd.org.rs/JSCS

UDC 546.47'73:544.642.076.2:
544.654.2:620.193

Original scientific paper

Microstructure and corrosion behaviour of Zn–Co alloys deposited from three different plating baths

JELENA B. BAJAT^{1*}, SANJA I. STEVANOVIĆ^{2#} and BOJAN M. JOKIĆ^{1#}

¹Faculty of Technology and Metallurgy, University of Belgrade, Karnegijeva 4, 11120 Belgrade and ²ICTM – Institute of Electrochemistry, University of Belgrade, Njegoševa 12, 11001 Belgrade, Serbia

(Received 31 March, revised 4 July 2011)

Abstract: The effects of plating baths of different composition on the microstructure and corrosion stability of Zn–Co alloy coatings were studied. Zn–Co alloys with the same Co content were deposited from chloride plating baths containing different amounts of Co^{2+} , as well as from a sulphate–chloride plating bath. The surface morphology and crystallite size were investigated by scanning electron microscopy (SEM) and atomic force microscopy (AFM). The corrosion stability of the Zn–Co alloys was determined by following the change of the open circuit potential with time of immersion in a 3 % NaCl solution and by polarization measurements. The results showed a significant influence of the plating bath on the morphology and corrosion stability of the Zn–Co alloys. The surface of the alloy coatings deposited from the chloride baths were uniform and homogenous, whereas the deposit obtained from the sulphate–chloride bath was quite inhomogeneous. The corrosion stability of the homogenous Zn–Co deposits obtained by deposition from both chloride baths was higher than that of the deposit obtained from the sulphate–chloride bath. An increase in the Co content in the chloride-plating bath resulted in a reduction of the alloy crystallite size and it was shown that the alloy with the smaller crystallites of the two alloy deposits, although having the same chemical content, exhibited a lower corrosion rate.

Keywords: electrodeposition; coatings; Zn–Co alloy; corrosion; AFM.

INTRODUCTION

The electrodeposition of zinc alloy coatings has been of interest recently since these alloys provide better corrosion protection than pure zinc coatings.^{1–4} The alloying of Zn is easily achieved with more noble metals, mostly with metals of the iron group (Ni, Co and Fe).^{5–11} If zinc alloys have effectively a high

* Corresponding author. E-mail: jela@tmf.bg.ac.rs

Serbian Chemical Society member.

doi: 10.2298/JSC110331137B



amount of zinc, they can still maintain a sufficiently negative potential to steel and yet, offer better corrosion protection than zinc alone.⁹ It is stated in the literature that the main corrosion product for all zinc-coatings is zinc hydroxide chloride, $Zn_5(OH)_8Cl_2 \cdot H_2O$ (ZHC).^{4,6,11,12} According to the corrosion mechanism suggested by Lambert,¹³ zinc dissolves preferentially at the beginning of the corrosion process, providing galvanic protection to the steel. This, however, leads to an enrichment of the alloy with the nobler component (dezincification) and the alloy coating becomes a composite-like structure, consisting of corrosion products and a layer rich in the alloying elements. This newly formed coating acts as a protective barrier layer, which reduces the corrosion rate.^{10,13,14} This mechanism was confirmed by Short et al.¹⁴ for Zn–Co alloys containing 1–10 % Co.

It is known that, compared with Zn and other Zn alloys, Zn–Co alloys have other superior properties, namely hardness, ductility, internal stresses, paintability and weldability.^{15,16} Different plating baths for Zn–Co co-depositions are reported in the literature, giving deposits with varied properties.^{3,17–22} The different properties of alloy coatings depend on their structure and composition, whereby the structure and composition of an alloy coating are determined by the plating parameters. Some of these parameters are: temperature of the plating bath, the type of the bath, the deposition current density or the deposition potential and the deposition mode.^{23–25} Each of these parameters has its own influence on the structure and composition of an alloy coating, which, however, could often not be unambiguously defined, but are rather dependent on other plating parameters.

Since there are numerous publications related to Zn–Co alloy coatings having a low Co content (≈ 1 wt. %)^{5,7,11,12,15} and not many reported on Zn–Co alloys with higher Co contents, Zn–Co deposits with 6 wt. % Co were investigated in this work. The aim of this work was to study the effects of three different plating baths on the morphology of Zn–Co coatings and their corrosion stability. Namely, it would be of interest to investigate Zn–Co deposits having the same Co content but obtained from different plating baths, and to determine how the type of the plating bath affects the morphology and the corrosion stability of the obtained Zn–Co deposits.

EXPERIMENTAL

Electrodeposition of Zn–Co alloys

Zn–Co alloys were deposited galvanostatically on a steel or platinum panel from three different plating baths (Table I) at room temperature (25 ± 1 °C). The employed plating baths were free of additives since the aim of the study was to investigate only the influence of different deposition baths on the morphology and corrosion stability of Zn–Co deposits.

The electrolytes used were prepared using *p.a.* chemicals and high purity water (Millipore, 18 MΩ cm resistivity).

Deposition times were chosen to obtain Zn–Co deposits of 15-μm thickness.

The working electrodes for polarization measurements and open circuit potential measurements, as well as for scanning electron microscopy (SEM), atomic force microscopy (AFM)



and energy dispersive spectroscopy (EDS), were Zn–Co alloys deposited on a steel (ISO T57) panel. The steel substrates were pre-treated by mechanical cleaning (abrading successively with emery papers of the following grades: 280, 360, 800 and 1000) and then degreased in a saturated solution of sodium hydroxide in ethanol, pickled with a 1:1 hydrochloric acid solution for 30 s and finally rinsed with distilled water. For determining the chemical composition, Zn–Co alloys were additionally deposited on platinum panels, then dissolved in a small amount of HCl solution (1:1) (5–10 cm³) and the chemical composition was determined by atomic absorption spectroscopy. Prior to each electrodeposition, the Pt surface was mechanically polished with a polishing cloth (Buehler Ltd.) impregnated with an aqueous suspension of alumina powder (0.3 µm grade), and then rinsed with pure water in an ultrasonic bath.

TABLE I. Plating baths²⁶

Bath	Composition	$j_{\text{dep}} / \text{A dm}^{-2}$	pH
Chloride	0.1 mol dm ⁻³ ZnCl ₂	2	5.5
	0.03 or 0.5 mol dm ⁻³ CoCl ₂ ·6H ₂ O		
	0.4 mol dm ⁻³ H ₃ BO ₃		
	3 mol dm ⁻³ KCl		
Sulphate–chloride	0.24 mol dm ⁻³ ZnSO ₄ ·7H ₂ O	8	5.5
	0.1 mol dm ⁻³ CoSO ₄ ·7H ₂ O		
	0.32 mol dm ⁻³ H ₃ BO ₃		
	2.0 mol dm ⁻³ KCl		

The counter electrodes were a zinc panel placed parallel to a steel panel for the electrodeposition of the alloys, or a Pt panel for the polarization and corrosion measurements. The reference electrode used in all experiments was a saturated calomel electrode (SCE).

The plating parameters were chosen (Table I) so that all the alloy deposits had the same Co content (≈ 6 wt. %).²⁶

Corrosion measurements

The corrosion rates in aerated 3% NaCl solution (pH 6.7) of the electrodeposited Zn–Co alloys were determined using extrapolation of anodic polarization curves to the open circuit potential (OCP). A potential sweep rate of 0.2 mV s⁻¹ was applied starting from the OCP, after a constant OCP had been established. The cathodic and anodic polarization curves were recorded in two separate experiments.

Chemical composition and surface morphology

The surface morphology of different Zn–Co deposits was observed by a JEOL JSM 5800 scanning electron microscope (SEM). The chemical content of deposited alloys was determined using an Oxford System for Energy Dispersive Spectroscopy (EDS) connected to the SEM. In addition, the chemical composition of the Zn–Co alloys was determined by atomic absorption spectroscopy (AAS) using an AAS-PYE Unicam SP9, Philips instrument.

The morphological characterization was performed by atomic force microscopy (AFM) using a NanoScope 3D (Veeco, USA) microscope operated in the tapping mode under ambient conditions. Etched silicon probes with a spring constant of 20–80 N m⁻¹ were used.



RESULTS AND DISCUSSION

The effect of the plating bath on alloy deposition

Galvanostatic curves for deposition of Zn–Co alloys from different plating baths are presented in Fig. 1. It could be seen that the deposition potential greatly depends on both the type of the plating bath and the Co^{2+} content in the plating bath. Namely, the Zn–Co alloy deposited mainly at -1.22 V from the chloride bath containing the lower amount of Co^{2+} and the deposition potential advanced to a more noble value, -1.13 V, as the concentration of Co^{2+} in the bath increased. According to the Fig. 1, a higher overpotential was needed to create the initial nucleus during deposition from the bath with the lower Co^{2+} content. Similar results were reported for Zn–Ni deposition.²⁷ Plating from sulphate–chloride bath was performed at an even lower overpotential, -1.07 V, although the current density of electrodeposition was higher than in the cases of the chloride baths.

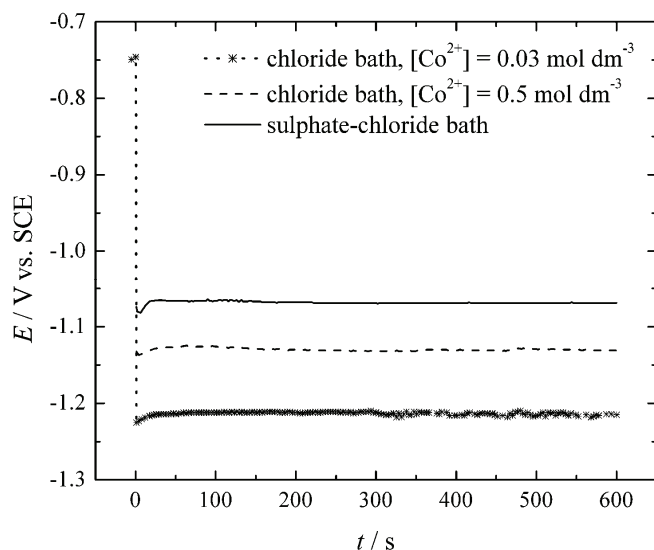


Fig. 1. Galvanostatic curves in different plating baths for the deposition of Zn–Co alloys.

The small potential fluctuation on the galvanostatic curves, especially pronounced for the curve related to Zn–Co deposition from the chloride bath with the lower amount of Co^{2+} , is the result of hydrogen evolution. Namely, the current efficiency for the electrodeposition of this alloy coating was the lowest (23 %)²⁶ as compared to 75²⁶ and 40 % for electrodeposition of Zn–Co coatings from the chloride bath with the higher amount of Co^{2+} and from the sulphate–chloride bath, respectively.

The differences in the deposition potentials from the two chloride baths were due not only to the different amounts of Co^{2+} , but also to the different ratios of

Co^{2+} to Cl^- in the two plating baths. Namely, different types of complexes could be formed in aqueous halide solutions, depending on the cobalt to chloride ions ratio.²⁸ In electrolytes with a large excess of Cl^- with respect to Co^{2+} , as it was the case in this work for the chloride plating bath with lower Co^{2+} content, at room temperature, it is considered that cobalt reactive species form complexes, CoCl_4^{2-} .²⁸ The $[\text{Cl}^-]/[\text{Co}^{2+}]$ ratio was very high (109) in this plating bath and, thus, electrodeposition was realized from complexes with the highest overpotential (Fig. 1). On the contrary, in plating baths with a low $[\text{Cl}^-]/[\text{Co}^{2+}]$ ratio, the reactive species are metal cations, Co^{2+} . The $[\text{Cl}^-]/[\text{Co}^{2+}]$ ratio was lower (≈ 8) for the chloride bath with the higher Co^{2+} content, which resulted in deposition with lower overpotential in respect to deposition from the other chloride bath. As a result of all the above-mentioned, the electrodeposition from the two different chloride plating baths resulted in deposits having the same amount of Co (≈ 6 wt. %) that were obtained at the same deposition current density, but at different overpotentials. The electrodeposition from sulphate–chloride plating bath was also performed at a low $[\text{Cl}^-]/[\text{Co}^{2+}]$ ratio, which was, however, more than two times higher (20) than in the chloride bath with the higher Co^{2+} content; hence, electrodeposition of the Zn–Co deposit with ≈ 6 wt. % Co from the sulphate–chloride plating bath was realized at a different current density and the lowest overvoltage.

Surface morphology

The surface morphology of electrodeposited Zn–Co alloys was investigated using SEM. SEM and optical microscopy have proved themselves to be convenient methods for the analysis of the surface morphology of electrochemical deposits^{29,30} and in determining the crystallite size in alloy deposits. SEM Images of Zn–Co alloys having the same Co content, but deposited from different plating baths, are shown in Fig. 2.

SEM Analyses of the morphology of the samples studied indicate clear difference between the deposits obtained from the different plating baths. The deposit obtained from the chloride bath with the lower Co^{2+} content is illustrated in Fig. 2a. The surface of this alloy coating is uniform, homogenous and consists of irregular crystals particles. The surface morphology of the Zn–Co alloy obtained from the plating bath with the higher Co^{2+} content in the plating bath, at the same current density, is shown in Fig. 2b. This deposit is also homogenous and uniform, with a dense surface morphology covering the entire surface area. EDS Analysis showed the same chemical content over both these alloy deposits. It could be seen that increasing the cobalt content in the plating bath resulted in a reduction of the crystallite size (Figs. 2a and 2b). However, the deposit obtained from the sulphate–chloride bath is quite inhomogeneous (Fig. 2c). The local differences in chemical content for this deposit were determined using EDS. Namely, the Zn–Co alloy deposit obtained from sulphate–chloride bath also con-



tained 6.0 wt. % Co, as determined by AAS. EDS Analysis, however, showed slight differences in the Co content in different areas of deposit, with the Co contents ranging from 5.7–8.3 wt. %. In addition, 3.0 % oxygen was also detected by EDS.

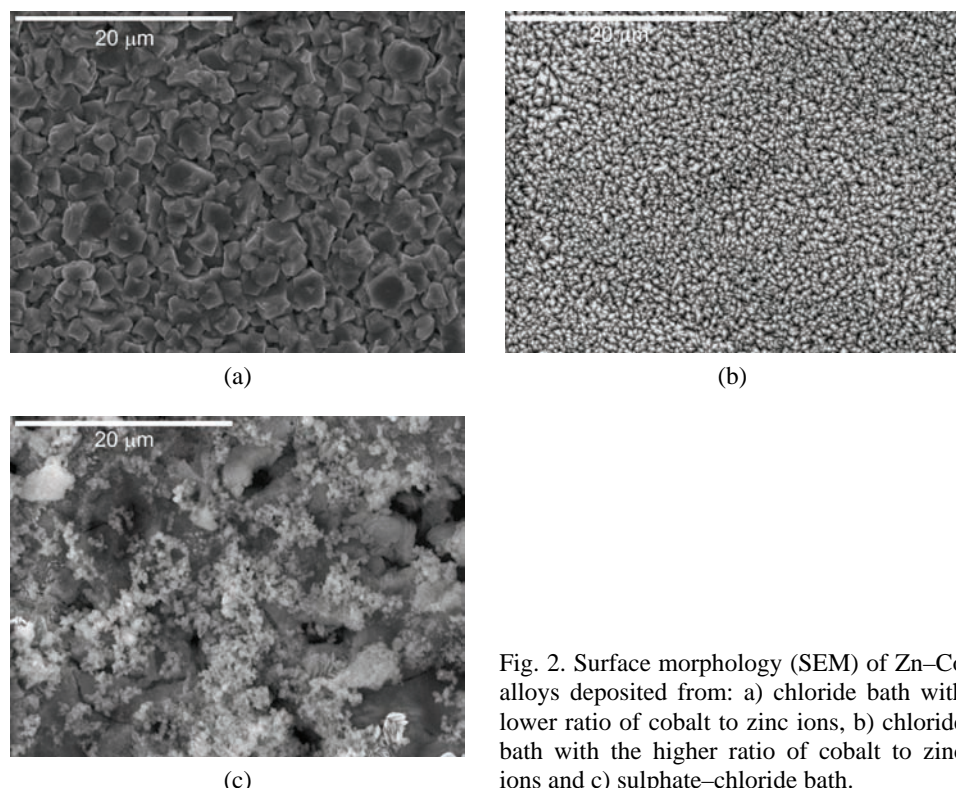


Fig. 2. Surface morphology (SEM) of Zn–Co alloys deposited from: a) chloride bath with lower ratio of cobalt to zinc ions, b) chloride bath with the higher ratio of cobalt to zinc ions and c) sulphate–chloride bath.

Corrosion stability

The effect of the plating bath on the corrosion stability of the Zn–Co alloys was determined by following the change of the open circuit potential, E_{OCP} , with time of immersion in a 3 % NaCl solution and by polarization measurements. The open circuit potential of the bare steel surface in 3 % NaCl was –640 mV *vs.* SCE and it is marked with the dotted line in Fig. 3. The potentials of the Zn–Co alloys were more negative than that of the steel base under the same conditions; thus, the Zn–Co alloys provide sacrificial cathodic protection. The OCPs of the alloys deposited from all three baths were initially almost the same, but over time, they increased positively at different rates and reached almost the same values (the steel E_{OCP}) after different time intervals, which represent loss of the coating and the start of the corrosion process.

The results of the visually observed alloy destruction in 3 % NaCl solution, or the appearance of red rust on the steel base, are presented in Table II. The

longest time before the appearance of red rust, indicating the best corrosion stability, was observed for Zn–Co alloy deposited from chloride bath with the higher Co^{2+} content, whereas the Zn–Co deposit obtained from the sulphate–chloride bath was destroyed the fastest.

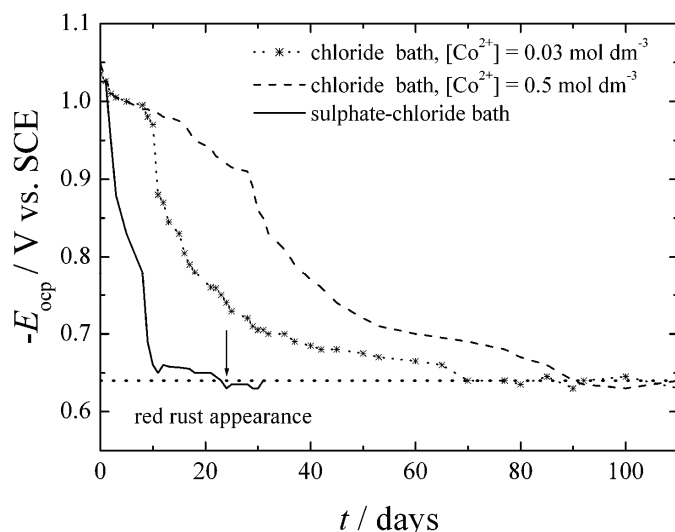


Fig. 3. The dependence of E_{ocp} for the Zn–Co alloys deposited on steel from different plating baths (15-μm thickness).

TABLE II. The time of red rust appearance and corrosion current densities, j_{corr} , for Zn–Co alloys deposited from different plating baths (all the data are mean values of 3–5 measurements)

Bath	Time, days	$j_{\text{corr}} / \mu\text{A cm}^{-2}$
Chloride, $[\text{Co}^{2+}] = 0.03 \text{ mol dm}^{-3}$	70	12
Chloride, $[\text{Co}^{2+}] = 0.5 \text{ mol dm}^{-3}$	92	3
Sulphate–chloride	23	40

In addition, polarization curves were obtained in a 3 % NaCl solution and are presented in the form of E –log j plots (Fig. 4). As can be seen, the anodic reaction is activation-controlled alloy dissolution, while the cathodic reaction is oxygen reduction under diffusion control. Thus, the corrosion current densities, j_{corr} , were determined from the intersect of the anodic Tafel plots with the OCP and the values are given in Table II. The data given in Table II are mean values of three to five measurements.

Since the amount of Co in alloy deposits was the same, the corrosion potential differs only slightly for all the alloy deposits. However, a clear difference among the samples could be seen from the potentiodynamic curves (Fig. 4). The corrosion rate of the deposit obtained by plating from the sulphate–chloride bath was

higher than the ones deposited from the chloride baths. The highest corrosion stability was observed for the Zn–Co alloy deposited from the chloride bath with the higher Co^{2+} content. These results are in agreement with the results of the appearance of red rust.

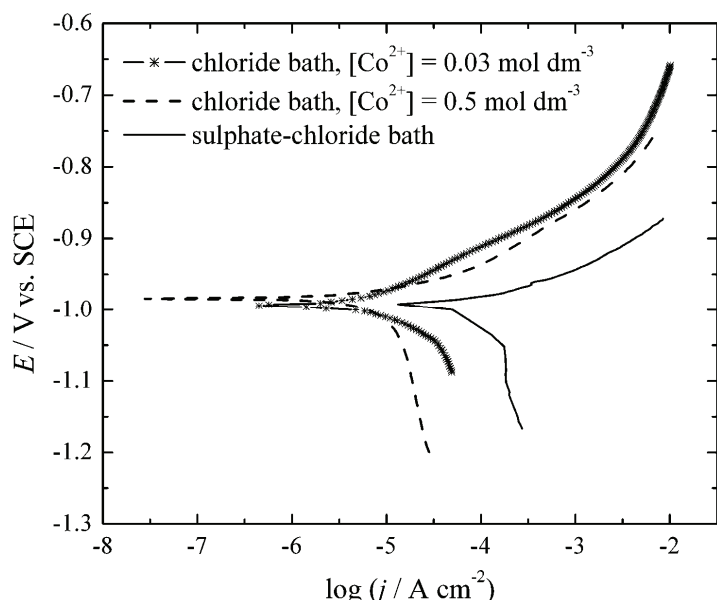


Fig. 4. Anodic polarization curves in 3 % NaCl for the Zn–Co alloys deposited from the different plating baths.

The differences in corrosion properties among the different Zn–Co alloys arise from the different surface morphology obtained by deposition from the different plating baths. Namely, it is well known that Zn coatings deposited from baths of various compositions have differences in porosity, structure and other characteristics, which, in turn, affect the corrosion resistance of the coatings.⁹ It was shown in the literature that the phase composition of Zn–Co deposits is determined by their Co content.^{22,26,31,32} Zn–Co deposits with between 4 and 10 wt. % Co are composed of quasi-pure Zn and the $\text{Zn}_{21}\text{Co}_5$ γ phase.³¹ However, since all the investigated Zn–Co alloys contained 6 wt. % Co, it is supposed that all deposits had the same phase structure, and that the differences in corrosion stability arise from the different morphologies of the alloy deposits obtained from the different plating baths.

It was shown in the literature that deposits formed from chloride baths have less inorganic inclusions as compared to deposits from sulphate baths and the presence of inorganic inclusions, in turn, leads to higher corrosion rates.³³ The Zn–Co deposit obtained from the sulphate–chloride bath did contain 3 % of oxy-

gen (from oxide), as shown by EDS analysis. The inhomogeneous morphology of alloy deposit obtained from sulphate–chloride bath is probably another reason for the reduced corrosion stability of this alloy deposit (Figs. 2–4), since different amounts of Co in different areas of Zn–Co alloy deposit obtained from sulphate–chloride bath could lead to the galvanic coupling and, consequently, to a reduction of protective properties. Namely, the local microstructural variations of deposit (as can be seen in Fig. 2c, for Zn–Co deposit obtained from sulphate–chloride bath) adopt different equilibrium potentials in aqueous solutions and are thus, susceptible to local galvanic corrosion.³⁴

Therefore, it could be concluded that the type of the plating bath had a significant role in defining the surface properties, such as crystallite size, deposit homogeneity and distribution, as well as corrosion stability, of the alloys. From the SEM micrographs shown in Fig. 2, it could be seen that the Zn–Co alloys deposited from the chloride plating baths with the lower and higher Co^{2+} content have extremely different morphologies as compared to the surface morphology of the Zn–Co alloy deposited from the sulphate–chloride plating bath. It would be of interest to find out the reason for the better corrosion stability of the homogenous deposit obtained from the chloride-plating bath with the higher Co^{2+} content as compared to the also homogenous deposit obtained from the chloride-plating bath with the lower Co^{2+} content. The SEM micrographs showed the differences in morphology of the deposits obtained by deposition from those two chloride baths, and that larger crystallites were obtained for deposition from the bath with the low Co^{2+} content.

In order to gain a deeper insight into the surface morphologies of these alloy deposits, AFM images were taken. Typical three-dimensional (3D) and two-dimensional (2D) AFM images of the Zn–Co deposits obtained in the chloride plating bath with the lower Co^{2+} content are shown in Figs. 5a and 5b. The deposit is made up of crystallite agglomerations which are compact and uniformly cover the entire substrate. The 2D image of this deposit resembles very well the morphology shown in the corresponding SEM micrograph (Fig. 2a). The crystal agglomerations are of diverse dimensions, ranging from 1.5–2.5 μm (Fig. 5b).

The AFM images of the deposit obtained from the chloride plating bath with the higher Co^{2+} content reveal a completely different surface morphology with globular agglomerations (Figs. 6a and 6b). These globules are in the size range 0.7–2.0 μm (Fig. 6b), and are made up of smaller, nanosized crystallites in the 150–300 nm size range (Fig. 6b).

The chemical compositions of deposits shown in Figs. 5 and 6 were the same, but the increase of Co content in the plating bath resulted in a deposit having a smaller crystallite size. This globular surface morphology, in turn, resulted in improved corrosion stability. In addition, the deposit obtained from the chloride bath with the lower Co^{2+} content had a much coarser morphology than the one ob-



tained from the chloride bath with the higher Co^{2+} content. The finer grained structure of the Zn-Co alloy obtained from the chloride bath with the higher Co^{2+} content resulted in better corrosion stability, probably because the small grain size created a high-volume fraction of the boundaries that act as a corrosion barrier.³⁵ The deposition from the chloride bath with the lower Co^{2+} content resulted in larger crystallite sizes (Figs. 2, 5 and 6) and higher anodic dissolution (Figs. 3 and 4).

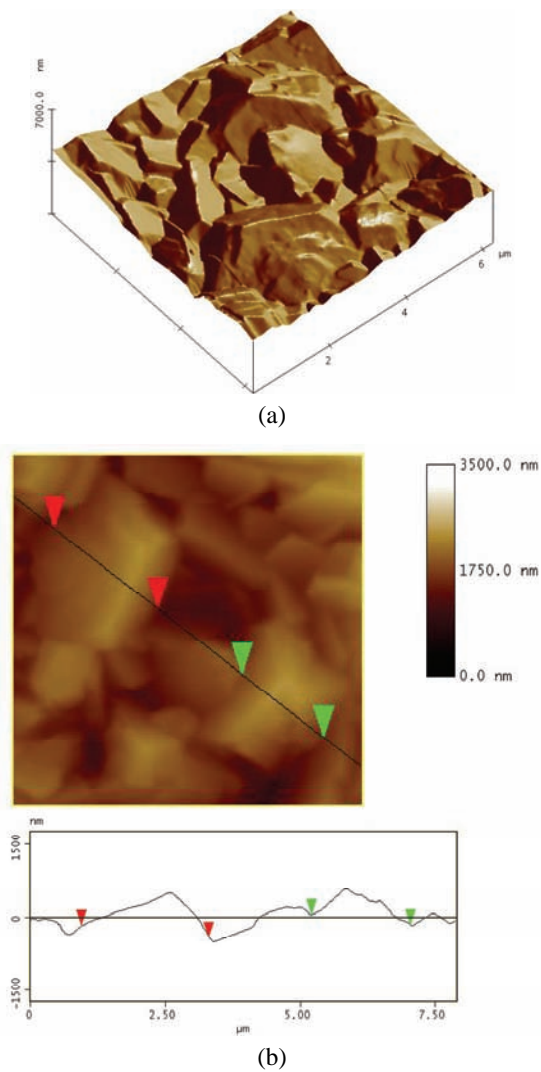


Fig. 5. a) 3D AFM Images ($5 \times 5 \times 3.5 \mu\text{m}^3$) and b) 2D AFM images and height profiles of the Zn-Co alloy deposited from the chloride bath with the lower cobalt content at 2.0 A dm^{-2} .

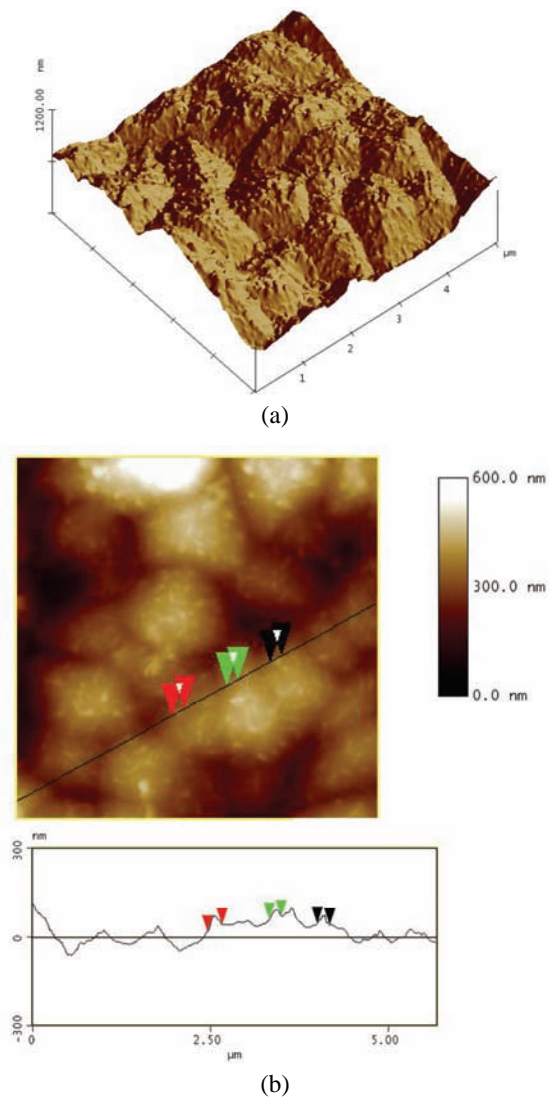


Fig. 6. a) 3D AFM Images ($5 \times 5 \times 3.5 \mu\text{m}^3$) and b) 2D AFM images and height profiles of the Zn–Co alloy deposited from the chloride bath with the higher cobalt content at 2.0 A dm^{-2} .

Another reason for the increased corrosion stability of the Zn–Co alloy coating deposited from the chloride bath with the higher Co^{2+} content could be related to the greater current efficiency obtained during deposition from this bath. Namely, when hydrogen evolution, as a parallel reaction occurring at the cathode, is immense, the hydrogen bubbles formed could be partly incorporated in the alloy deposit. Since the current efficiency was more than three times smaller for the deposition from the chloride bath with the lower Co^{2+} content, these alloy

coatings are probably more susceptible to corrosion, as compared to the deposits obtained from the chloride bath with the higher Co^{2+} content.

CONCLUSIONS

Based on the results presented, it could be concluded that the type of the plating bath has a significant influence on the morphology, as well as, on the corrosion stability of electrodeposited Zn–Co alloys.

The surfaces of the alloy coatings deposited from the chloride baths, determined by SEM, were uniform and homogenous, whereas the deposit obtained from the sulphate–chloride bath was quite inhomogeneous. The corrosion stability of the Zn–Co deposits obtained by deposition from both chloride baths was higher than that of the deposit obtained from the sulphate–chloride bath.

The inhomogeneous deposit obtained from the sulphate–chloride bath with oxygen inclusion resulted in reduced corrosion stability, namely the highest corrosion current density, as well as the shortest time before the appearance of red rust. However, the homogenous and dense surface morphology of the Zn–Co deposit obtained from the chloride-plating bath with a higher Co^{2+} content resulted in increased protective properties.

The increase of the cobalt content in the chloride-plating bath resulted in a reduction in the crystallite size of the alloy and an increase in the current efficiency of the alloy deposition. It was shown that the alloy with the smaller crystallite grains of the two alloy deposits obtained from the chloride-plating baths having the same chemical content yielded a lower corrosion rate.

Acknowledgement. This research was financed by the Ministry of Education and Science of the Republic of Serbia, Contract No. III 45019.

ИЗВОД

МИКРОСТРУКТУРА И КОРОЗИОНО ПОНАШАЊЕ Zn–Co ЛЕГУРА ТАЛОЖЕНИХ ИЗ СУЛФАТНОГ И ХЛОРИДНИХ РАСТВОРА

ЈЕЛЕНА Б. БАЈАТ¹, САЊА И. СТЕВАНОВИЋ² и БОЈАН М. ЈОКИЋ¹

¹Технолошко–мештапарски факултет, Универзитет у Београду, Карађорђева 4, 11120 Београд и

²ИХТМ – Центар за електрохемију, Универзитет у Београду, Његошева 12, Београд

У овом раду је проучаван утицај врсте раствора за таложење на микроструктуру и корозиону стабилност превлака Zn–Co легура. Zn–Co легуре са истим садржајем Co су електрохемијски таложене из хлоридних раствора са различитим садржајем јона кобалта, као и из сулфатно–хлоридног раствора. Морфологија површине превлака је испитивана скенирајућом електронском микроскопијом и микроскопијом атомских сила. Корозиона стабилност превлака Zn–Co легура је одређивана праћењем промене потенцијала отвореног кола са временом деловања раствора NaCl концентрације 3%, као и поларизационим мерењима. Добијени резултати су показали значајан утицај врсте раствора за таложење на морфологију и корозиону стабилност превлака Zn–Co легура. Превлаке Zn–Co легура добијене из хлоридних раствора су хомогене, док су превлаке добијене из сулфатно–хлоридног раствора нехомогене. Корозиона стабилност превлака легура добијених из оба хлоридна раствора је већа у



односу на стабилност легура добијених из сулфатно-хлоридног раствора. Повећањем садржаја кобалта у хлоридном раствору за таложење добијају се превлаке мањих кристалита и у раду је показано како величина кристалита утиче на корозиону стабилност легура са истим садржајем кобалта.

(Примљено 31. марта, ревидирано 4. јула 2011)

REFERENCES

1. I. H. Karahan, *J. Mater. Sci.* **42** (2007) 10160
2. S. R. Rajagopalan, *Met. Finish.* **70** (1972) 52
3. M. Pushpavanam, S. R. Natarajan, K. Balakrishnan, L. R. Sharma, *J. Appl. Electrochem.* **21** (1991) 642
4. M. H. Gharahcheshmeh, M. H. Sohi, *Mater. Chem. Phys.* **117** (2009) 414
5. R. Ramanauskas, R. Juskenas, A. Kalinichenko, L. F. Garfias-Mesias, *J. Solid State Electrochem.* **8** (2004) 416
6. C. N. Panagopoulos, D. A. Lagaris, P. C. Vatista, *Mater. Chem. Phys.* **126** (2011) 398
7. N. Boshkov, K. Petrov, S. Vitkova, S. Nemcska, G. Raichevsky, *Surf. Coat. Technol.* **157** (2002) 171
8. J. B. Bajat, A. B. Petrović, M. D. Maksimović, *J. Serb. Chem. Soc.* **70** (2005) 1427
9. M. A. Pech-Canul, R. Ramanauskas, L. Maldonado, *Electrochim. Acta* **42** (1997) 255
10. W. Kautek, M. Sahre, W. Paatsch, *Electrochim. Acta* **39** (1994) 1151
11. R. Ramanauskas, L. Gudaviciute, L. Diaz-Ballote, P. Bartolo-Perez, P. Quintana, *Surf. Coat. Technol.* **140** (2001) 109
12. R. Fratesi, G. Roventi, C. Branca, S. Simoncini, *Surf. Coat. Technol.* **63** (1994) 97
13. M. R. Lambert, G. R. Hart, H. E. Townsend, *Corrosion mechanism of Zn-Ni alloy electrodeposited coatings, SAE Tech. Pap. Series No. 831817*, Detroit, MI, 1983, p. 81
14. N. R. Short, A. Abibsi, J. K. Dennis, *Trans. Inst. Met. Finish.* **67** (1989) 73
15. P.-Y. Chen, I.-W. Sun, *Electrochim. Acta* **46** (2001) 1169
16. A. Stankevičiute, K. Leinartas, G. Bikulcius, D. Virbalyte, A. Sudavicius, E. Juzeliunas, *J. Appl. Electrochem.* **28** (1998) 89
17. M. S. Chandrasekar, S. Srinivasan, M. Pushpavanam, *J. Solid State Electrochem.* **13** (2009) 781
18. C. N. Panagopoulos, K. G. Georgarakis, S. Petroutzakou, *J. Mater. Process. Tech.* **160** (2005) 234
19. R. D. Srivastava, R. C. Mukerjee, *J Appl. Electrochem.* **6** (1976) 321
20. F. Elkhatabi, M. Benballa, M. Sarret, C. Muller, *Electrochim. Acta* **44** (1999) 1645
21. S. Swathirajan, *J. Electrochem. Soc.* **133** (1986) 671
22. J. B. Bajat, S. Stanković, B. M. Jokić, *J. Solid State Electrochem.* **13** (2009) 755
23. J. Y. Fei, G. D. Wilcox, *Electrochim. Acta* **50** (2005) 2693
24. K. A. Prasad, P. Giridhar, V. Ravindran, *J Solid State Electrochem.* **6** (2001) 63
25. J. B. Bajat, M. D. Maksimović, G. R. Radović, *J. Serb. Chem. Soc.* **67** (2002) 625
26. J. B. Bajat, S. Stanković, B. M. Jokić, S. S. Stevanović, *Surf. Coat. Tech.* **204** (2010) 2745
27. M. M. Abou-Krisha, F. H. Assaf, A. A. Toghan, *J. Solid State Electrochem.* **11** (2007) 244
28. H. Ma, C. Wan, A. H. Zewall, *PNAS* **105** (2008) 12754



29. A. T. Dimitrov, P. Paunović, O. Popovski, D. Slavkov, Ž. Kamberović, S. Hadži Jordanov, *J. Serb. Chem. Soc.* **74** (2009) 279
30. N. D. Nikolić, V. M. Maksimović, M. G. Pavlović, K. I. Popov, *J. Serb. Chem. Soc.* **74** (2009) 689
31. E. Gomez, X. Alcobe, E. Valles, *J. Electroanal. Chem.* **505** (2001) 54
32. Z. F. Lodhi, F. D. Tichelaar, C. Kwakernaak, J. M. C. Mol, H. Terryn, J. H. W. de Wit, *Surf. Coat. Techn.* **202** (2008) 2755
33. L. Felloni, R. Fratesi, E. Quadrini, G. Roventi, *J. Appl. Electrochem.* **133** (1987) 574
34. Z. F. Lodhi, J. M. C. Mol, A. Hovestad, L. 't Hoen-Velterop, H. Terryn, J. H. W. de Wit, *Surf. Coat. Techn.* **203** (2009) 1415
35. G. B. Hamu, D. Eliezer, L. Wagner, *J. Alloys Comp.* **468** (2009) 222.

